ϕ, ρ and ω production in collisions induced by deuteron and heavy ions at 200 GeV per nucleon

Denis Jouan[8] for the NA50 and NA38 collaboration:

M.C. Abreu[6], C. Alexa[2], B. Alessandro[11], J. Astruc[8], C. Baglin[1], A. Baldit[4], F. Bellaiche[12], M. Bedjidian[12], S. Beole[11] A. Borhani[9], V. Boldea[2], G. Bonazzola[11], P. Bordalo[6], A. Bussière[1], V. Capony[1], J. Castor[4], M. Cerú[3], T. Chambon[4], B. Chaurand[9], I. Chevrot[4], B. Cheynis[12], E. Chiavassa[11], C. Cicalo[3], S. Constantinescu[2], W. Dabrowski[11], A. De Falco[3] G. Dellacasa[11], N. De Marco[11], A. Devaux[4], S. Dita[2], O. Drapier[12], B. Espagnon[4], J. Fargeix[4], F. Fleuret[9], P. Force[4], M. Gallio[11], Y.K. Gavrilov[7], C. Gerschel[8], P. Giubellino[11], M.B. Golubeva[7], M. Gonin[9], P. Gorodetzky[10], J.Y. Grossiord[12], P. Guaita[11], F.F. Guber[7], A. Guichard[12], R. Haroutunian[12], M. Idzik[11], D. Jouan[8], T.L. Karavitcheva[7], R. Kossakowski[1], L. Kluberg[9], A.B. Kurepin[7], Y. Le Bornec[8], G. Landaud[4], C. Lourenço[5], L. Luquin[4], P. Macciotta[3], F. Ohlsson-Malek[12], A. Marzari-Chiesa[11], M. Masera[11], A. Masoni[3] , S. Mourgues[4], A. Musso[11], P. Petiau[9], W.L. Prado da Silva[11a], A. Piccotti[11], J.R. Pizzi[12], G. Puddu[3], C. Racca[10], L. Ramello[11], S. Ramos[6], P. Rato-Mendes[11], L. Riccati[11], A. Romana[9], P. Saturnini[4], E. Scomparin[11], R. Shaoian[5], S. Silva[6], S. Serci[3], P. Sonderegger[5], X. Tarrago[8], P.Temnikov[3], N.S. Topilskaya[7], G. Usai[3], E. Vercellin[11], and N. Willis[8].

[1] L.A.P.P., F-74019, Annecy-le-Vieux, France
[2] IFA, Bucharest, Romania.
[3] Università di Cagliari/INFN, Cagliari, Italy.
[4] L. P. C., F-63177 Aubière Cedex, France
[5] CERN, CH-1211 Geneva 23, Switzerland
[6] LIP, Av. E. Garcia, 14-1, P-1000 Lisbon, Portugal
[7] INR, Moscow, Russia.
[8] I.P.N, F-91406 Orsay, France
[9] Ecole Polytechnique, L.P.N.H.E, F- 91128 Palaiseau, France
[10] C.R.N, F-67037 Strasbourg, France
[11] I.N.F.N., I-10125 Torino, Italy
[12] I.P.N., F-69622 Villeurbanne, France
[a] Now at UERJ, Rio de Janeiro, Brazil

Abstract. The production of low mass dimuons has been measured in d-C, d-U and S-U collisions at 200 GeV per nucleon, and in Pb-Pb collisions at 160 GeV per nucleon. The ϕ, ρ and ω productions in S-U collisions[1, 2] are extracted from a new set of data with increased statistic, and are through $\phi/(\omega+\rho)$ ratio compared to first results on deuteron induced production. These new analysis are presented in the limited M_T domain of recent Pb-Pb measurement whose preliminary results are also presented.

1 Introduction

The NA38 experiment measures muon pair production in coincidence with the transverse energy produced in ultrarelativistic heavy ion collisions. Thanks to a geometrical model of the collision and in the framework of the Bjorken model [3], one can relate this transverse energy to the energy density reached in the collision. This energy density is found sufficient to reach the critical temperature T_c [4] of the phase transition toward a plasma of quarks and gluons (QGP). A possible signature of this phase transition could be the J/ψ suppression [5] due to the screening effect of the plasma on the $c\bar{c}$ pair. This effect has been observed [6], but is already qualitatively present in proton nucleus reactions and is thus an ambiguous signature of the QGP formation. Recently, the continuity of this suppression when increasing the size of the participant regions[7] has been disturbed by the results of the Pb-Pb measurements[8]. Interpretations of this phenomenon are still matter of discussions, and this brings more interest in looking to the remaining informations of the dimuon spectrum.

In this work we will focus on the low mass part, observing another possible signature of the QGP[9, 10], linked to the general strangeness enhancement which has been also observed in several experiments [11]. Beyond the interest as another direct QGP signature, this is a combination of different signatures recorded in the same experimental conditions, that could constraint more strongly the models and eventually lead to inconsistencies in the purely hadronic description, which could be the ultimate signature of the QGP formation.

2 Experimental set up

The NA38/NA50 detector [6] consists mainly of a muon spectrometer made of an absorber followed by tracking chambers and hodoscopes upstream and downstream a toroidal magnet. An electromagnetic calorimeter measures the neutral transverse energy produced, which is related to the impact parameter of the collision. Target and beam detectors also prevent pile up biases in these high intensity measurements (see Table 1.)

In order to improve the mass resolution as compared to first results [12], some changes were done in the materials immediately following the target [1, 2].

Beam	Inten.	Target	Observation	$\mu\mu$(ana.)	S/D
d 200 GeV	610^8	C 11 cm	no calo	326205	0.78
d 200 GeV	610^8	U 2 cm	no calo	588952	0.76
S 200 GeV	410^7	U 1 cm	12 targets	1144540	.34-.7
Pb 160 GeV	510^6	Pb .7 cm	7 targets B $\times$ 7/4	1846869	.25-.5

Table 1:
Beams and targets,
including intensity per burst and signal over
signal+background (S/D) in the ω region

- for S-U measurements the inner part of the calorimeter was replaced by Al_2O_3,and for Pb-Pb by BeO.
- for deuteron induced collisions there was no calorimeter, and the target was a simple cylinder of matter.
- the Pb-Pb setup was optimised for J/ψ measurements, with an increased field in the magnet which was suppressing the low transverse momenta for the low masses (table 2 and figure 1).

It has to be noted also that for Pb beam (NA50) the beam and target detectors have been rebuilt in order to be adapted to the more difficult radiation conditions, and a silicon multiplicity counter and a zero degree calorimeter have been added. The beam energy is decreasing for Pb, so the spectrometer has been set to a different aperture angle, corresponding in both cases to a rapidity domain between 0. and 1. in the center of mass of the nucleon-nucleon collision.

Thanks to some of these improvements the mass resolution is about 75 MeV/c^2. The precision on the ϕ peak position could then not be better than several per cent, due to the statistic available, but also to the effect of continuum and other resonances, to the 50 MeV/c^2 mass binning, and the overall precision on the energy loss in the absorber.

As compared to proton, the deuteron beam has several interesting features: isospin similar to sulfur, and high intensity (Table 1.) beams can be used at SPS at the same energy than sulfur ones. Deuteron is then an ideal reference for ion studies, that can be obtained in rather short time (1 week here).

Pb-Pb results are very preliminary, and various comparisons are still under way between the different analysis done in NA38 and NA50. Only ratios $\phi/(\rho + \omega)$ will then be considered in this study, and no temperature will be extracted at this stage. Moreover no extrapolation to kinematical domains outside the acceptance will be done, in particular namely the low M_t domain. only M_t domains where the

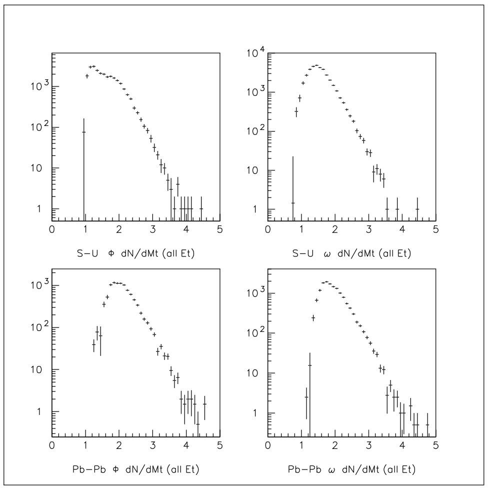

Figure 1: Transverse mass distribution for ϕ and ω mass regions,in Pb-Pb and S-U collisions, displaying the effect of the change in magnetic field of the spectrometer.

acceptance is at least on the percent level will be considered here.

$M_t(Gev/c^2)$		0.9-1.2	1.2-1.5	1.5-1.8	1.8-2.2	2.2-2.5	2.5-2.8	2.8-3.2
S-U	ω	0.30	2.05	5.35	7.15	9.76	5.9	5.34
	ϕ	0.72	1.78	3.47	7.25	6.52	8.74	8.72
Pb-Pb	ω			0.172	.83	1.56	1.5	1.44
	ϕ			0.10	.87	2.12	2.92	3.21

Table 2: Acceptances (%) in various M_T bins, calculated for $0 < Y < 1$ and $-1 < \cos\theta < 1$

The acceptances are very small for masses below the ω one. Studies of the low mass continuum is then more difficult than in other dilepton experiment [13, 14]

3 Background subtraction

The number of different pairs that can be made with N_+ positive mesons is simply $N_{++} = N_+(N_+ - 1)/2$, whereas the number of possible combinations with the N_- negative mesons is $N_{+-} = N_+ N_-$.

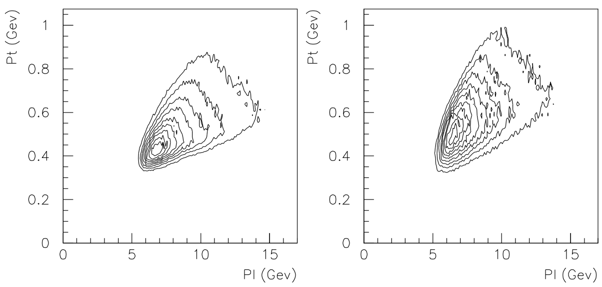

Figure 2: $P_L - P_T$ distribution of + and - single muons (without image cut).

These relations are valid for averaged quantities, if the distributions are Poissonian and N^+ and N^- are uncorrelated. This gives the normalisation of the combinatorial background originating from the uncorrelated decays of mesons into muon, or even mixing between different events, with the formula:

$< N_{+-} >= 2\sqrt{< N_{++} >< N_{--} >}$.

This formula can also be used for differential quantities, provided the two distributions are proportional. Acceptances are in fact very different for the different charges, as shown in Fig. 2, and in order to fulfill this condition, a selection was done on the tracks (image cut).

4 Extracting the different components

We are then aiming at extracting the resonances, in the mass spectra corresponding to physical windows of interest. In this analysis the continuum is only given a phenomenological shape fitted on the experimental spectrum, in order to improve the precision in the extraction of resonances.

4.1 Acceptance and smearing

Acceptance and resolution (smearing) have to be taken into account in analysis of the the dimuon mass spectra. Both effects are estimated through a complete Monte Carlo of the experiment, in which simulated tracks are reconstructed using the same procedure as for experimental data. There are two ways of extracting the corrected components ϕ, ρ, ω from the mass spectra:

- correct for smearing (eventually also for acceptance) the experimental mass spectrum, then fit it with physical (PPDB) mass shapes,
- fit the experimental uncorrected spectrum with "measured" simulated distributions of the various components.

Both methods are in principle equivalent, with nevertheless different levels of difficulty in estimating the associated error. The iterative process leading to the smearing correction indeed contains a certain amount of determination of the components.

Finally one gets the numbers of ϕ, ρ, ω *produced* in the kinematical available domain (M_T bin, $0. < Y_{cdm} < 1.$, $-0.75 < \cos\theta < 0.75$), from the one *measured* in the same domain, with an implicit correction for the balance of the exchanges between adjacent domains.

In this study we use the second method, after an initial step for tuning the simulated kinematical distributions in regard of the experimental ones.

4.2 Kinematical variable

The choice of the meaningful parameters used for representing the phenomenon is naturally linked to the subsequent use, or even to the interpretation, foreseen. In this analysis we have chosen to study the mass spectra in windows of the transverse mass M_T instead of the transverse momentum P_T.

Since M_T is the final variable used for temperature determination then it is more consistent to consider it throughout the whole data analysis, at least once to look for eventual systematic biases. Furthermore an M_T scaling is expected, whereas on the contrary the P_T distribution is known to change with the dimuon mass [15]. Looking at the ratio $\phi/(\rho+\omega)$ in different M_T windows would anyway give a direct information about M_T scaling.

On the other hand, mass spectra in limited M_T domains displays a variety of shapes, and are then more sensitive to the relationship between the the M_T spectra associated to the various component (Fig. 3).

4.3 Simulation of the mass, M_T and Y distributions

For the continuum, a phenomenological mass distribution is considered,
$dN/dM_{\mu\mu} \propto (\frac{1}{M_{\mu\mu}})^{\alpha} \exp -\beta M_{\mu\mu}$, with $\alpha = 3$ and $\beta = .9$.

The ρ is a broad resonance, its shape then depends on the available phase space [16] which is also responsible for the above exponential falling of the continuum. As in previous studies [12] the Breit-Wigner distribution has thus been multiplied by $1/M_{\mu\mu}^4$ in order to avoid unphysical infinite tails.

Simulated distribution are initially generated according to
$dN/dM_T \propto M_T^{-3/2} K_1(M_T/T)$ with T arbitrarily fixed to 180 MeV (230MeV for PbPb), and the Y distribution is taken as a Gaussian. M_T and Y simulated spectra for the various components are then compared to the experimental spectra obtained in similar mass domains, for instance $0.65 < M < 0.85$ GeV/c^2 for ω and $.95 < M < 1.1$ GeV/c^2 for ϕ .

The observed ratio between simulated and experimental distribution is fitted with an ad hoc function, which is here the ratio between a transverse mass distri-

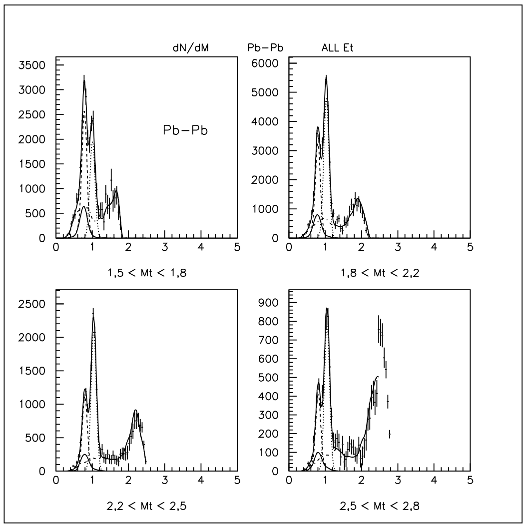

Figure 3: Examples of fit of mass spectra in various M_T bins.

bution as above, and the one obtained from a $dN/dP_T \propto P_T \exp -a \times P_T$. This correction is applied to source (i.e. before smearing) variables, and is found effective in limiting the differences below 20%.

4.4 Sensitivity of acceptance determination

Changing ingredients of the simulation changes the acceptance and then the results. To estimate the systematic uncertainties and their correlations, the major ingredients have been modified. The effect on the observables ϕ and ω is displayed in Table 3 . The overall effect is on the level of some per cent for $\phi/(\rho+\omega)$ ratio, for $M_T > 1.8 GeV/c^2$.

5 Results

Fig. 4 displays d-C, d-U and S-U data that have been taken in close experimental conditions, whereas the Pb-Pb mass spectrum shows the effect of the lowering of the acceptance for low masses, associated to an increase of the transverse masses threshold. The mass fits are also shown and reproduce well the data, even high statistic d-C and d-U ones.

Fig. 5 displays the $\phi/(\rho+\omega)$ obtained from these analysis in the M_T windows considered. These results are preliminary and have been restricted to domains

$M_T (Gev/c^2)$		1.2-1.5	1.5-1.8	1.8-2.2	2.2-2.5	2.5-2.8
ingredient	observable			effect (%)		
contin. shape	$\omega + \rho$	-5	+3	+5	+7	+7
$(\alpha - 0.5)$	ϕ	-10	+7	+3	+4.	+4
contin. shape	$\omega + \rho$	-1.	-2	-4	-5	-5
(β -0.2)	ϕ	+4	+1	-3	-4	-5
ρ shape	$\omega + \rho$	+0.6	0.	-0.4	-0.3	-.03
$(1/m^4 \to 1/m^3)$	ϕ	-2.5	-2	-2.	-0.6	-0.4
-10% θ_{ms}	ϕ or ω	+5.5	+4	+3	+2	+1.5
sim M_T shape	ω	0.2	0.4	0.7	0.9	0.7
(T -10 MeV)	ϕ	0.51	0.1	0.4	0.8	0.5
BCKG (-10%)	$\omega + \rho$	+5	+3	+2	+1	+0.1
	ϕ	+9	+6	+4	+2	+1.

Table 3:
Variations as a function of various ingredients
(θ_{ms} characterises the multiple scattering).

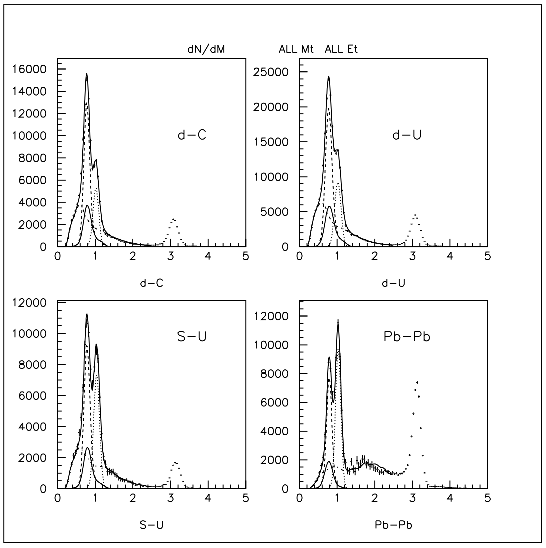

Figure 4: Fit of mass spectra for various collisions, for all measured transverse masses.

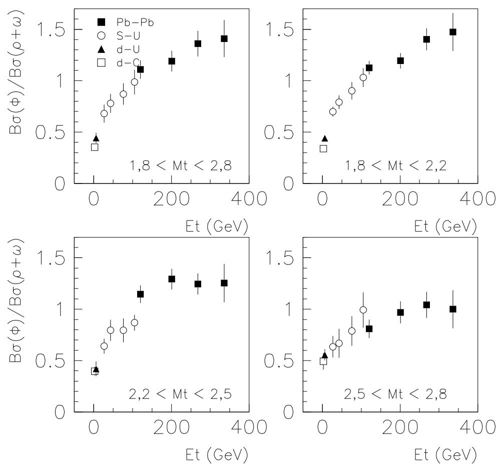

Figure 5: Evolution of $\phi/(\omega+\rho)$ as a function of the transverse energy, for various M_T domains.

of higher acceptances and statistics. These $\phi/(\rho+\omega)$ values cannot be directly compared to other experiments since they require to be extrapolated to low M_T, which is beyond the scope of this preliminary study, and anyway questionable in the limited domain of Pb-Pb measurements.

Various neutral transverse energy E_T^0 bins have been considered for S-U and Pb-Pb results. Fig. 5 displays $\phi/(\rho+\omega)$ for the four systems as a function of E_T^0 . The choice of this variable, which compares somehow with the number of hadrons used in other experiments, is mainly for convenience, particularly between S-U and Pb-Pb where the measured Pb-Pb E_T^0 spectra do not agree with the extrapolations from S-U, suggesting that E_T^0 could be 20% overestimated in Pb-Pb. Other variables such as the equivalent thickness L, the surface of the participant zone or the energy density could be more meaningful parameters, less related to the volume. Then the regular pattern with respect to E_T^0 must be taken with care, being probably coincidental. Nevertheless there is a clear increase as a function of the system and also as a function of the impact parameter.

Fig. 6 shows the same effect, integrated on impact parameter and as a function of the numbers of nucleons. The increase between d-C and d-U is smaller than between d-U, S-U and Pb-Pb, with respect to A_pA_t. As already noticed[1, 2], proton and ion induced collisions displays different behaviours. One see that it is still true between deuteron and ion, even for Pb results. The enhancement of

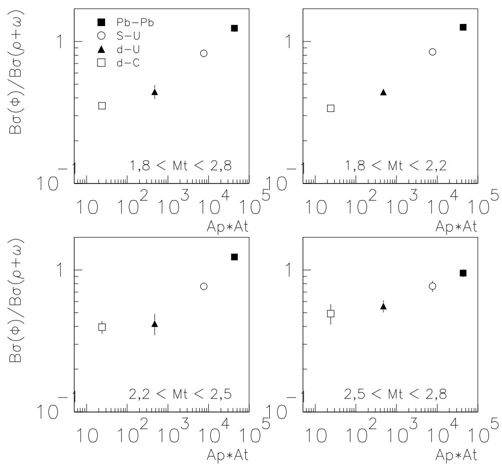

Figure 6: Evolution of $\phi/(\omega+\rho)$ as a function of $A_p \times A_T$, for various M_T domains.

$\phi/(\rho+\omega)$ typical to heavy ion collisions shows no saturation with lead projectile, but on the contrary from d-U to Pb-Pb it follows a power law as a function of A_pA_t.

6 Conclusions

These result are preliminary, they aim at a first comparison between Lead, Sulfur and deuteron induced collisions. Various checking are still under way, and only part of the available data is considered.

Only the ratio $\phi/(\rho+\omega)$ is considered, on a limited M_T range between 1.8 and 2.8 GeV/c^2. In this domain, there is a continuous enhancement of the strangeness production when going from deuteron to sulfur, and then from sulfur to lead induced reactions. Unlike for the ratio K_0 over hadrons [17], there is no saturation of strangeness production between sulfur and lead, but an increase of the same order of magnitude as the one between deuteron and sulfur. Although pure hadronic descriptions of this enhancement are considered [18, 20, 19] it is compatible with a quark gluon plasma scenario [21]. The observed additional enhancement is also another hint of a change in the conditions reached in these Pb-Pb collisions compared to the sulfur ones, which could be related to the cause of the dramatic suppression of J/ψ production observed in the same experiment [8].

References

[1] C.Baglin et al., *Physics Letters B* **368** (1996) 230-238

[2] C.Baglin et al., *Physics Letters B* **368** (1996) 238-243

[3] J.D.Bjorken, *Phys. Rev. D* **27** (1983) 140

[4] F.Karsch, *Nucl. Phys. A* **590** (1995) 367c.

[5] H.Satz, *Nucl. Phys. A* **590** (1995) 63c.

[6] C.Baglin et al., *Physics Letters B* **220** (1989) 471

[7] C.Gerschel and J.Hufner, *Z. Phys.C* **56** (1992) 171.

[8] M.Gonin et al., NA50 collaboration, to be published in proceedings of the Quark Matter conference, Heidelberg, May 20-24 1996

[9] A.Shor, *Phys. Rev.* **54** (1985) 1122

[10] P.Koch, B.Muller, J.Rafelski, *Phys. Rep.* **142** (1986) 167.

[11] G.Odyniec, Intriguing aspects of strangeness production at CERN energies, in this conference

[12] C.Baglin et al., *Physics Letters B* **272** (1991) 449-454

[13] P.Wurm et al., NA45 collaboration, *Nucl. Phys. A* **590** (1995) 103c.

[14] M.Masera et al., Helios/3 collaboration, *Nucl. Phys. A* **590** (1995) 93c.

[15] K.Kinoshita, H.Satz and D.Schildknecht, *Phys. Rev. D* **17** (1978) 1834.

[16] J.D.Jackson, *Nuovo Cimento* **34A** (1964) 1644.

[17] P.G.Jones et al., NA49 collaboration, to be published in proceedings of the Quark Matter conference, Heidelberg, May 20-24 1996

[18] P.Koch, U.Heinz and J.Pišút, *Phys. Lett.* **243** (1990) 149
P.Koch, U.Heinz and J.Pišút, *Z. Phys. C* **47** (1990) 477

[19] H.Sorge, *Nucl. Phys. A* **590** (1995) 571c

[20] F.Grassi and H.Heiselberg, *Phys. lett. B* **267** (1991) 1.

[21] H.W.Barz, B.L.Friman, J.Knoll and H.Schulz, *Phys. Lett B* **259** (1991) 162